Physical Phenomena and Porosity Prevention Mechanism in Laser-Arc Hybrid Welding†

KATAYAMA Seiji*, NAITO Yasuaki**, UCHIUMI Satoru** and MIZUTANI Masami***

Abstract

Hybrid welding of stainless steels or aluminium alloys was performed with the heat sources of YAG laser and TIG, or YAG laser and MIG, respectively. The effects of welding conditions and melt flows on penetration depth, geometry and porosity formation were investigated with the X-ray transmission real-time observation method. Melt flows on penetration depth and geometry were consequently confirmed. Concerning porosity suppression, in TIG-YAG hybrid welding of stainless steel, no formation of bubbles was attributed to the absence of pores. On the other hand, disappearance of bubbles from the concave molten pool surface due to the arc pressure played an important role in reducing porosity in YAG-MIG hybrid welding of aluminium alloys at high arc currents.

KEY WORDS: (Hybrid welding), (YAG laser), (TIG), (MIG), (Penetration), (Melt flows), (Bubbles), (Porosity), (Stainless steel), (Aluminium alloy)

1. Introduction

Hybrid welding with YAG laser and TIG or MIG is receiving considerable attention all over the world since it possesses many advantages such as increased penetration, improved gap and misalignment tolerance, increased welding speed, enhanced process stability, and reduced porosity.[1-12)]

However, it seems that the physical phenomena and the mechanisms concerning penetration and porosity suppression are not fully understood. The melt flows and porosity generation/suppression mechanisms have not been observed during hybrid welding.

In this study, therefore, YAG laser-TIG arc and YAG laser-MIG arc hybrid welding were performed on Type 304 stainless steel plate with low S content and A5052 aluminium alloy plate, respectively. The effects of welding conditions on the weld bead penetration and geometry, surface roughness and quality, and porosity formation were investigated concerning welding directions, the distances between the laser-focused point and the TIG electrode or MIG wire target, and the TIG or MIG currents. To interpret their effects, droplet transfers from a filler wire to the molten pool and the flows of ZrO_2 particles on the puddle surface were observed during hybrid welding with a high-speed video. The keyhole behaviour, bubble formation and disappearance situation leading to porosity formation, the movement of W particles and the stirred situation of Pt wires were also observed through X-ray transmission real-time imaging system.

2. Materials Used and Experimental Procedures

2.1 Materials used

The materials used in hybrid welding with YAG laser and TIG arc heat sources are mainly Type 304 austenitic stainless steel of 10 mm in plate thickness, possessing the chemical compositions of 18.2%Cr-8.1%Ni-0.05%C-0.47%Si-0.99%Mn-0.028%P-0.003%S. The utilization of the steel with low S content ensures that the chief melt flows from high to low temperatures in the pool should occur due to the force driven by surface tension.

In hybrid welding with YAG laser and MIG arc heat sources, A5052 aluminium alloy plates of 2 to 4 mm in thickness and A5356 MIG wire of 1.2 mm in diameter were used to understand normal hybrid welding results and phenomena.

† Received on May 12, 2006
* Professor
** Former Graduate Students
*** Technical Official

Transactions of JWRI is published by Joining and Welding Research Institute, Osaka University, Ibaraki, Osaka 567-0047, Japan

2.2 Welding procedures

Hybrid welding with YAG laser and TIG arc or YAG laser and MIG arc was performed on the plates of Type 304 steel or A5052 alloy, as shown in **Figs. 1** and **2**, respectively. The welding heat sources used are a YAG laser machine (the maximum power P_0 = 4 kW), TIG welder (the maximum current: 300 A) with a W-2% Ce_2O_3 electrode of 3.2 mm in diameter and MIG welder (the maximum current: 350A) in the DCEP pulsed arc mode. An Ar-O_2 mixed gas was supplied from the coaxial nozzle (50 l/min) in YAG laser and TIG arc hybrid welding. After the chamber was filled with the mixed gas, the bead-on-plate welding experiments were performed in pure Ar shielding gas supplied from the TIG torch nozzle (30 l/min).

In this paper, backward welding with a YAG laser beam following and forward welding with a YAG laser beam leading are called TIG-YAG or MIG-YAG and YAG-TIG or YAG-MIG welding, respectively. The effect of distances (d) between the laser beam central axis and the TIG electrode tip and between the beam center axis and MIG wire target was investigated in YAG-TIG and YAG-MIG welding.

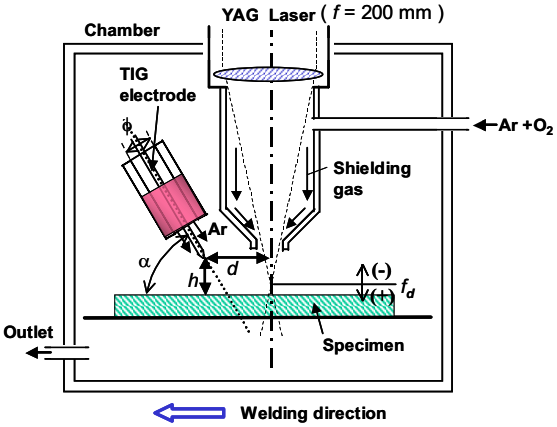

Fig. 1 Chamber producing pure Ar and Ar-O_2 mixture atmospheres and schematic experimental setup in YAG laser and TIG arc hybrid welding.

2.3 X-ray transmission real-time observation method of inside molten pool during welding

The penetration and porosity formation tendency of weld beads were investigated by optical microscope and X-ray inspection method. Moreover, keyhole behavior, bubble/porosity formation or disappearance, melt flows and molten pool geometry were observed through X-ray real-time transmission system. The system is schematically shown as an example of YAG-TIG welding in **Fig. 3**. For clearer visualization of molten pool geometry, a platinum (Pt) or tin (Sn) wire was placed in a hole on the surface of Type 304 or A5052 aluminum alloy plate, respectively. Tungsten (W) particles were also set to elucidate melt flows in the pool. The video framing speed was 500 or 1000 frames/s.

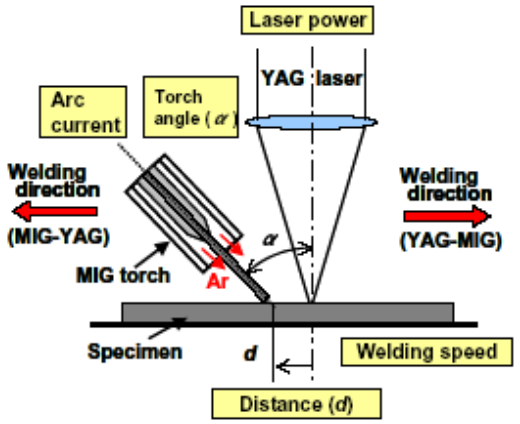

Fig. 2 Schematic experimental setup for YAG laser and MIG arc hybrid welding.

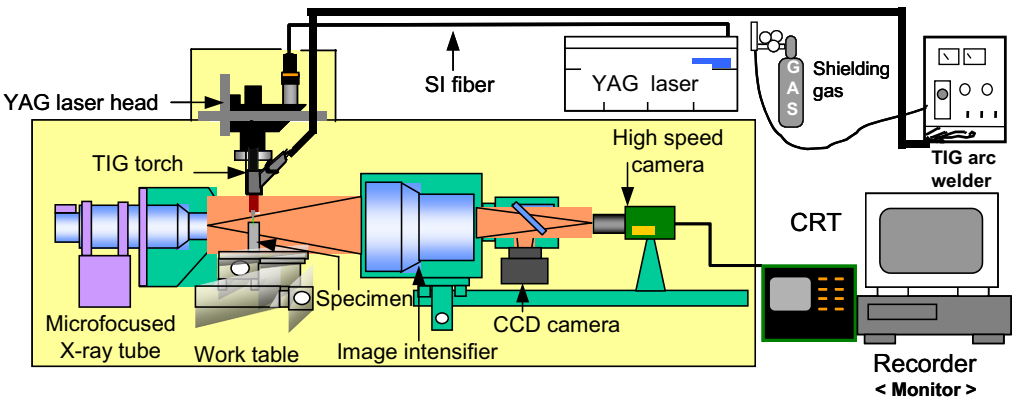

Fig. 3 Schematic arrangement of X-ray transmission imaging system for observation of phenomena inside molten pool during hybrid welding.

3. Experimental Results and Discussion

3.1 Hybrid welding results with TIG and YAG laser

The effect of the ambient atmosphere on penetration was investigated during welding with a YAG laser only or TIG-YAG hybrid in the atmosphere of Ar-oxygen mixed gas. The cross sections of weld beads are shown in **Fig. 4**, together with those produced in air without the chamber, for comparison. The numbers are the oxygen contents measured in the weld beads. The oxygen contents were larger with an increase in the oxygen gas ratio and in the air. In pure Ar atmosphere the weld beads showed a "nail head" type of geometry, but in the YAG laser welding and in the hybrid welding at 100A, the surface widths decreased and the penetration depths increased with an increase in the oxygen ratio or content. Especially it was confirmed that the oxygen affected the weld geometry and the "nail head" disappeared in the atmosphere of higher oxygen ratio or at higher O content. On the other hand, in the hybrid welding at the arc current of 200A, the penetration didn't become deep but the "nail head" part was wider and deeper with an increase in the oxygen gas ratio in the atmosphere. At any arc current, the weld beads produced in the air were similar to those in the atmosphere of higher oxygen ratio. This indicates that the oxygen gas in the atmosphere or high oxygen content should affect the laser and hybrid weld bead geometry.

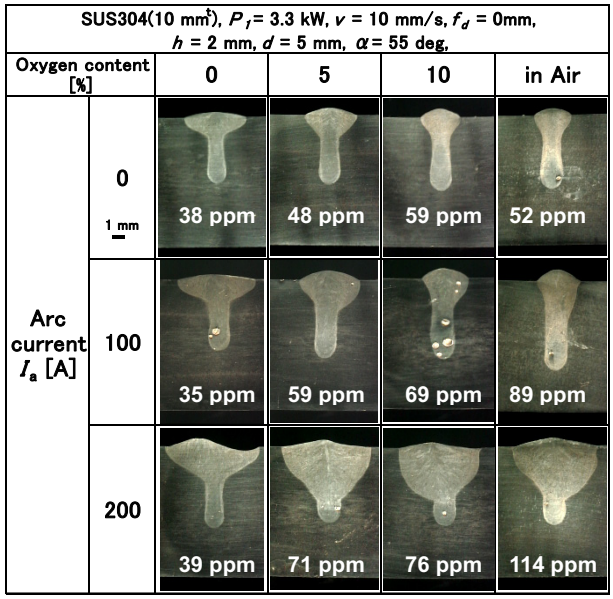

O content in base plate: 41 ppm

Fig. 4 Effects of arc current and environmental atmosphere on penetration geometry of laser and hybrid weld beads.

The X-ray inspection results of the respective weld beads are shown in **Fig. 5**. The amount of porosity increased in the weld metals at 100A but decreased at 200A. It was revealed in hybrid welding that porosity tendency was dependent upon the welding conditions, especially the TIG arc current.

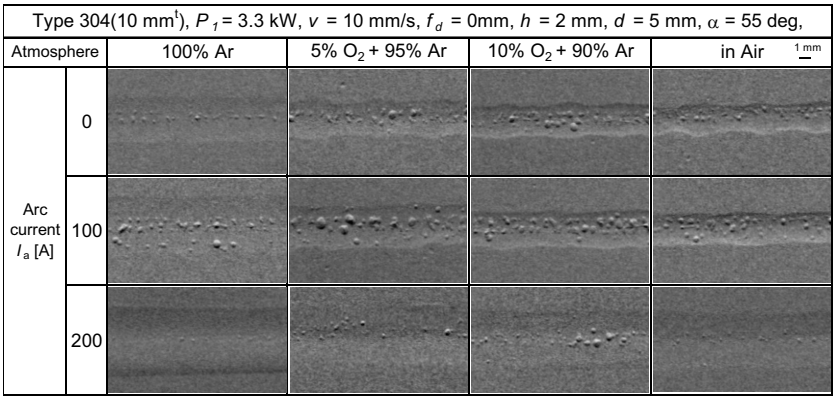

Fig. 5 X-ray inspection results of laser and hybrid weld beads, showing porosity formation tendency.

High speed video and X-ray transmission in-situ observation were carried out in laser and hybrid welding of Type 304 plate to gather actual information of keyhole behaviour, bubble and porosity formation or disappearance, and melt flows on the surface and inside the molten pool using specimens with ZrO_2 particles and Pt or W makers.

Figure 6 shows the effect of the arc current on weld penetration, porosity formation tendency, keyhole behaviour, and bubble generation in Type 304 steel with low S content. The phenomena of hybrid welding in the air at 100 and 200 A are schematically summarized in **Fig. 7**. In the YAG laser welding, bubbles were generated from the bottom part of the keyhole probably due to intense evaporation of metal or keyhole collapse. The bubbles were trapped by the solidifying front, resulting in the formation of porosity. At 100 A, a keyhole was slightly larger and deeper than that in

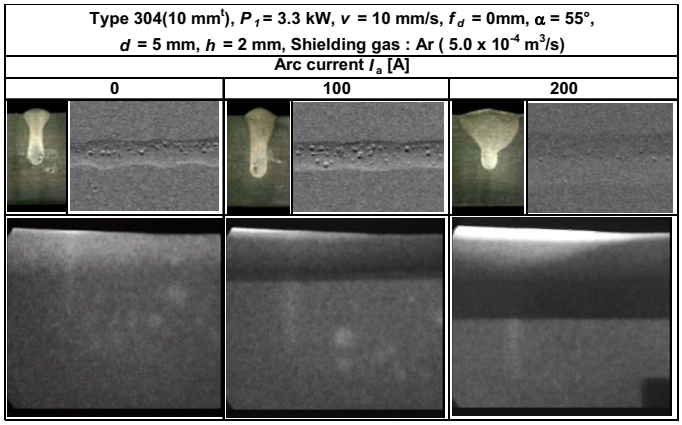

Fig. 6 Cross sections, X-ray inspection results and X-ray transmission in-situ observation results of Type 304 steel with low S content subjected to YAG laser only and hybrid welding at TIG arc currents of 100 and 200 A.

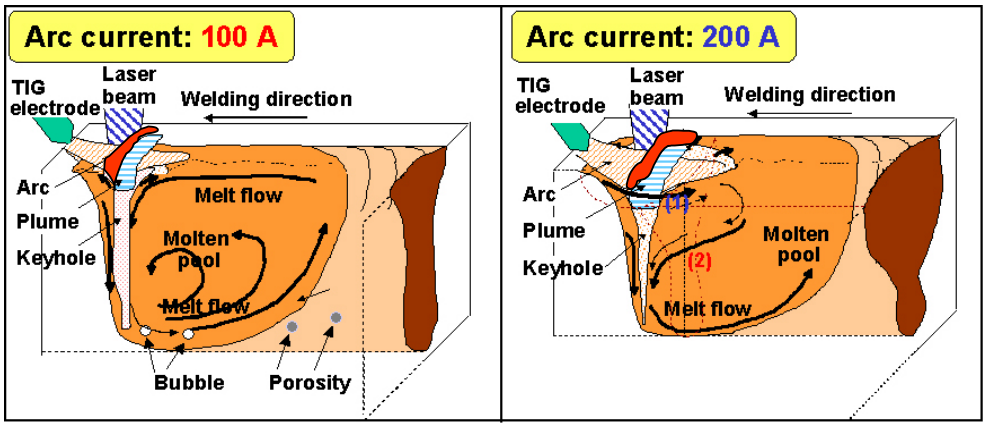

Fig. 7 Schematic representation of TIG-YAG hybrid welding phenomena, showing keyhole, plume, concave surface, melt flows inside molten pool leading to weld geometry.

YAG laser welding, and the downward flows of the melt near the keyhole wall were clearly seen, and thereafter the melt flowed from the keyhole tip to the rear along the bottom of the molten pool. This suggests that the latter flow along the bottom of the molten pool to the rear mainly deepens the molten pool. On the other hand, at 200A, the molten pool was depressed, the keyhole diameter near the top of the surface was larger, and other fast melt flows were observed around the keyhole near the surface, resulting in the formation of wider bead widths. It was also confirmed that the keyhole inlet became wider with an increase in the arc current. At 100 A, the diameter of the keyhole became slightly larger, but the formation of bigger bubbles increased in the formation of the porosity. At 200 A, the diameter at the top part of the keyhole was larger than that at 100 A, and the surface of the molten pool was heavily concave. Moreover, only a few bubbles were generated in the molten pool. It was revealed that bubble formation tendency depended upon the arc current. Porosity reduction at 200 A is attributed to the reduced bubble generation, but not to the disappearance of bubbles from the molten pool surface in YAG and TIG hybrid welding of Type 304 steel.

3.2 Hybrid welding results with YAG laser and MIG

YAG-MIG and MIG-YAG hybrid welding were carried out on A5052 alloy. Slightly easier melting or higher speed for full penetration welding was achieved in MIG-YAG welding. Good and bad surface appearances of weld beads were observed in YAG-MIG and MIG-YAG hybrid welding, respectively. Therefore, YAG-MIG and MIG-YAG hybrid welding may be recommended from the weld bead surface appearances and from the penetration, respectively.

YAG-MIG hybrid welding was performed at various MIG currents. The surface appearances, cross sections and X-ray inspection results of weld beads are shown in **Fig. 8**. The weld beads were wider and deeper with an increase in the MIG current. Porosity was reduced with increasing the MIG current, and it was almost absent at 240 A.

Formation and flow of bubbles resulting in pore formation were observed with the X-ray transmission observation method. Examples of X-ray transmission images during hybrid welding at 120 A and 240 A are exhibited in **Fig. 9**. Many bubbles were formed from the bottom of the keyhole during laser welding and hybrid welding at 120A. At 120A, the majority of them were trapped at the solidifying front of the weld fusion zone resulting in the formation of porosity. Such tendency was the same with the single YAG laser welding. At 240 A, on the other hand, the molten pool produced with a laser beam was strongly pushed down by

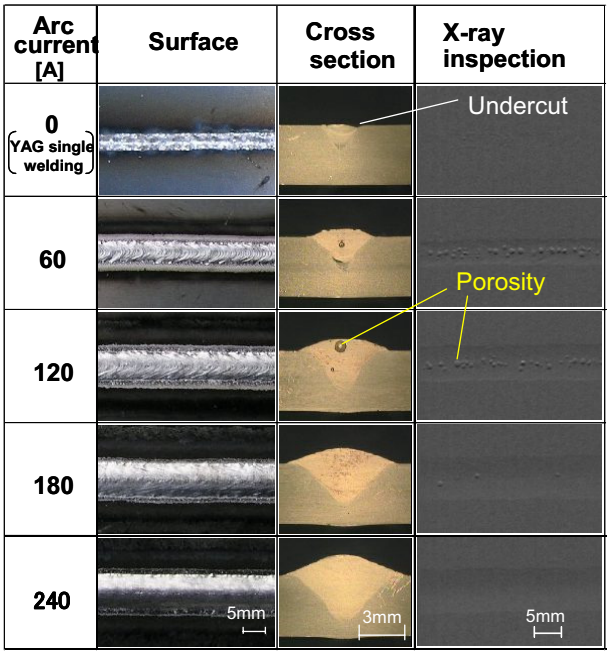

Fig. 8 Surface appearances, cross sections and X-ray inspection results of YAG laser and YAG-MIG hybrid weld beads.

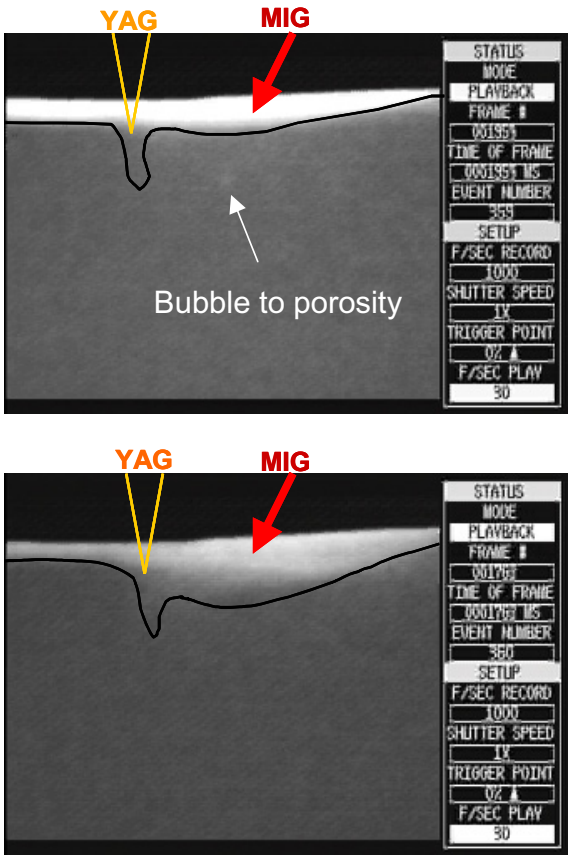

Fig. 9 X-ray transmission images during hybrid welding at 120 and 240 A, showing bubble generation leading to porosity and concave surface, respectively.

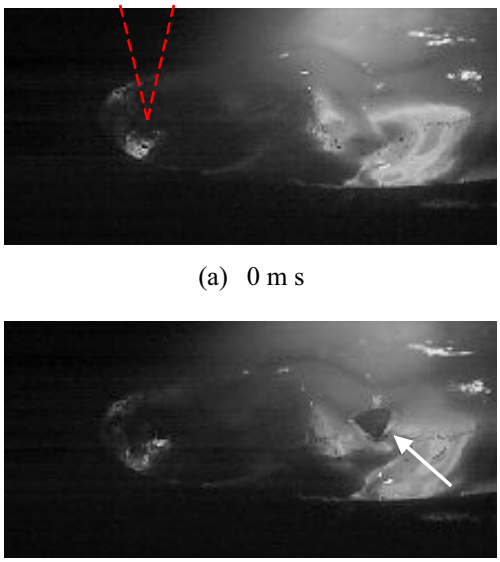

(a) 0 m s

(b) 0.1 ms

Fig. 10 High-speed video images of molten surface during hybrid welding, showing disappearance of bubble from rear central surface.

the MIG arc pressure to produce a concave surface. Consequently, the majority of bubbles generated from the keyhole disappeared into the atmosphere through the molten pool surface depressed by arc pressure. Such disappearance of bubbles from the pool surface was confirmed by the high-speed video observation result of a molten puddle during hybrid welding, as exhibited in **Fig. 10**.

The keyhole and molten pool geometry during YAG single welding (0 A) and hybrid welding at 120 and 240 A are schematically illustrated in **Fig. 11**. It was confirmed that the molten pool became large and long backward and could be easily suppressed with increasing the MIG current. The suppressed concave surface of the molten pool may be the reason for porosity reduction due to the disappearance of bubbles at high MIG currents.

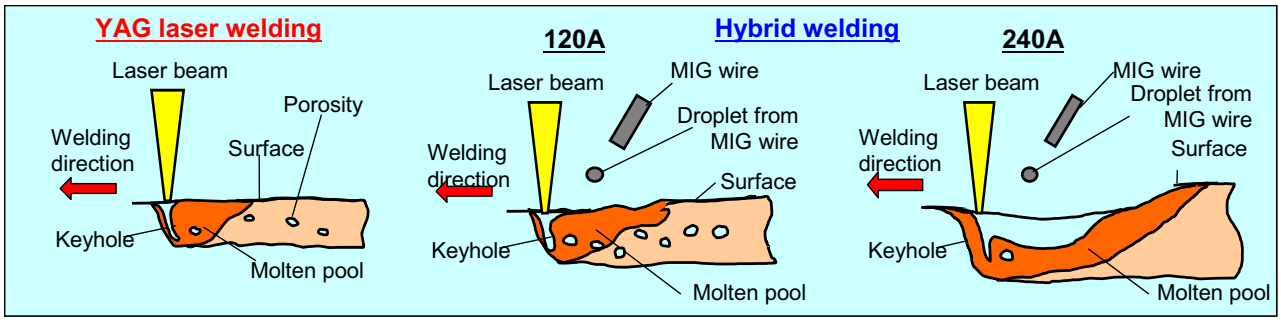

Fig. 11 Schematic representation of YAG laser and YAG-MIG hybrid welding phenomena, showing keyhole and bubble generation resulting in porosity during laser and hybrid welding at 120 A, and concave surface of molten pool leading to no porosity at 240 A.

4. Conclusions

The following conclusions are derived from the experimental results and discussion of YAG-TIG and YAG-MIG hybrid welding.

i) Concerning YAG-TIG welding of stainless steel;

(1) It was confirmed in both laser and hybrid welding of a steel with low S content that the penetration and geometry of weld beads depended upon the volume of the oxygen in the ambient atmosphere, and that a pronounced "nail head" disappeared in the atmosphere of higher oxygen ratio as well as in the normal air atmosphere.

(2) It was revealed that bubble and porosity formation tendency depended upon the arc current. In the hybrid welding at 100 A, the porosity increased in comparison with that in the laser welding and in the hybrid welding at 200 A.

(3) Especially at 200 A, the top diameter of the keyhole inlet was slightly wider and the surface of the molten pool was concave due to the strong gas stream stress or arc pressure, and moreover only a few bubbles were generated in the molten pool, resulting in reduced porosity or no porosity.

ii) Concerning YAG-MIG welding of aluminium alloy;

(1) The surface appearances were better in YAG-MIG welding; but on the other hand, the penetration was deeper in MIG-YAG welding.

(2) The penetration increased with an increase in the MIG current.

(3) In YAG-MIG hybrid welding, porosity could be reduced in number with increasing the MIG current and were absent at 240 A.

(4) The reason for the reduced porosity at higher MIG currents was attributed to the disappearance of bubbles from the suppressed molten pool surface according to the X-ray real-time transmission observation and high speed video observation.

Acknowledgements

The authors would like to acknowledge Dr Jing-Bo WANG and Mr. Kouji FUJII working for Matsushita Welding System Co. Ltd., and Associate Prof. Hidetoshi FUJII working for JWRI for their assistance in YAG-MIG hybrid welding and oxygen analyses, respectively. Part of the results was obtained under the joint project with KITECK, Korea. Further thanks would be expressed to Prof. Kiyoshi NOGI, Director General of JWRI, for financial support.

References

1) V. M. Steen and M. Eboo: “Arc augmented laser beam welding, Metal Construction”, **7-**7(1979), 332-335.

2) E. Beyer, U. Dilthey, R. Imhoff, C. Majer, J. Neuenhahn and K. Behler: “New aspects in laser welding with an increased efficiency”, *Proc. of ICALEO ’94*, Orlando, LIA, (1994), 183-192.

3) T. Ishide, S. Tsubota, M. Watanabe and K. Ueshiro, “Latest MIG, TIG arc-YAG laser hybrid welding system”, *Journal of the Japan Welding Society*, **72**-1(2003), 22-26.

4) T. Ishide, S. Tsubota and M. Watanabe: “Latest MIG, TIG arc-YAG laser hybrid welding systems for various welding products”, *Proc. of SPIE (First Int. Sym. on High Power Laser Macroprocessing)*, Osaka, JLPS, **4831** (2002), 347-352.

5) D. Petring, C. Fuhrmann, N. Wolf and R. Poprawe: “Investigation and applications of laser-arc hybrid welding from thin sheets up to heavy section components”, *Proc. of the 22nd Int* Congress *on Applications of Lasers & Electro-Optics (ICALEO)*, Jacksonville, LIA, (2003), Section A, 1-10 (CD:301).

6) N. Abe, Y. Kunugita and S. Miyake: “The mechanism of high speed leading path laser-arc combination welding”, *Proc. Of ICALEO '98*, Orlando, LIA, **85** Section F (1998), 37-45.

7) H. Staufer: “Laser hybrid welding & laser brazing at VW and Audi”, *Proc. of 6th High Energy Research Committee*, HiDEC-2003-01, (2003), 1-10.

8) J. Tsuek and M. Suban: “Hybrid welding with arc and laser beam”, *Science and Technology of Welding and Joining*, **4**-5 (1999), 308-311.

9) E. Beyer: “Laser technology for new markets –Application Highlights-“, 6th International *Laser Marke place 2003*, Anwendung im Dialog (2003) S. 5-15.

10) M. Kutsuna and L. Chen: “Interaction of Both Plasma in CO_2 Laser-MAG Hybrid Laser-hybrid Welding of Carbon Steel”, *IIW*, (2002), Doc.XII-1708-02.

11) E. Schubert, B. Wedel and G. Kohler: “Influence of the process parameters on the welding results of laser-GMA welding”, *Proc. of ICALEO 2002 (Laser Materials Processing Conference)*, Scottsdale, LIA, (2002) Session A-Welding (CD).

12) Y. Naito, M. Mizutani and S. Katayama: “Observation of keyhole behavior and melt flows during laser-arc hybrid welding”, *Proc. of the 22nd Int* Congress *on Applications of Lasers & Electro-Optics (ICALEO) 2003*, Jacksonville, LIA, (2003), (CD: 1005).